Tampereen yliopisto

Emma Pesu

DIFFERENTIATION AND CHARACTERIZATION OF DRAVET PATIENT DERIVED INDUCED HUMAN PLURIPOTENT STEM CELL LINE INTO CORTICAL NEURONS

Faculty of Medicine and Health Technology
Bachelor's thesis
April 2022

ABSTRACT

Emma Pesu: Differentiation and characterization of Dravet patient derived induced human pluripotent stem cell line into cortical neurons
Bachelor's thesis
Tampere University
Degree Programme in Biotechnology and Biomedical Engineering
April 2022

Dravet Syndrome is a severe infantile-onset epilepsy syndrome with often fever-triggered convulsive episodes and varying co-morbidities causing cognitive deficits and motor abnormalities. The cause of this neurodevelopmental disorder is mutations in *SCN1A* gene encoding the α-subunit of the type I voltage gated sodium channel Nav1.1. Sodium channels regulate the initiation and propagation of action potentials in neurons and therefore are responsible of information transmission in neuronal networks and throughout the brain. The loss of function of sodium channels due to mutations can lead to dysregulated action potential firing in cortical GABAergic inhibitory interneurons which regulate the activity of excitatory neurons. Decreased cortical inhibition causes imbalance of excitatory to inhibitory neurotransmission in neuronal networks that results in epileptic seizures.

The spontaneous network level activity of neurons can be studied using microelectrode arrays (MEAs) that are well plates with embedded microelectrodes in the bottom of the well. Yet, most of the electrophysiological studies used to model Dravet Syndrome using mouse models are performed at the single-cell level. Although these kinds of studies are important in determining molecular factors of disease pathogenesis, they do not describe how the network level function is affected in Dravet syndrome and in humans. Thus, there is a need for human-specific *in vitro* models that utilize human induced pluripotent stem cell (hiPSC)- derived neurons from patients and study the effects of these neurons on MEAs.

In the study, Dravet patient-derived hiPSC line and control hiPSC line were differentiated into cortical neurons and characterized at the gene and protein level using quantitative real-time PCR and immunocytochemical stainings. The produced neurons were plated on CytoView MEA well plates to record the spontaneous network level activity of the cells for a total of 8 weeks. The aim was to see and characterize the differences between pathological and normal healthy neuronal networks.

The results showed that cortical neuron differentiation was efficient in both cell lines, creating cells that had a mature neuron phenotype and were electrophysiologically active on MEAs. The expression of *SCN1A* gene was significantly lower in the patient cell line than in the control cell line. MEA analyses revealed significant difference in the network activity between the cell lines as the patient line derived neurons were less active during the measurements.

The information gained from this study can serve as a basis for future studies conducted with Dravet patient-derived hiPSC lines on MEAs. *In vitro* models using hiPSC-derived neurons to study the neuronal network function on MEAs are a promising research platform for epilepsies, including Dravet Syndrome. These human-specific disease models can further reduce the need and use of animal models.

Keywords: cortical neuron, Dravet syndrome, human induced pluripotent stem cells, microelectrode array, *SCN1A,* sodium channel

TIIVISTELMÄ

Emma Pesu: Dravet-potilasperäisen ihmisen indusoidun pluripotentin kantasolulinjan erilaistaminen aivokuoren neuroneiksi ja karakterisointi
Kandidaatintutkielma
Tampereen yliopisto
Bioteknologian ja biolääketieteen tekniikan tutkinto-ohjelma
Huhtikuu 2022

Dravetin oireyhtymä on vakava lapsuusiässä alkava epilepsia, johon liittyy usein kuumeen laukaisemia kouristuksia ja erilaisia samanaikaisia sairauksia, jotka aiheuttavat kognitiivisia puutteita ja motorisia poikkeavuuksia. Tämän hermoston kehityshäiriön syynä ovat mutaatiot *SCN1A*-geenissä, joka koodaa tyypin I jännitevälitteisen natriumkanavan Nav1.1 α-alayksikköä. Natriumkanavat säätelevät aktiopotentiaalien alkamista ja leviämistä neuroneissa ja ovat siksi vastuussa tiedonsiirrosta hermosoluverkostoissa ja koko aivoissa. Natriumkanavien toiminnan menetys-mutaatiot voivat johtaa säätelemättömään aktiopotentiaalien laukeamiseen aivokuoren GABA-välitteisissä inhiboivissa interneuroneissa, jotka säätelevät eksitatoristen neuronien toimintaa. Vähentynyt aivokuoren inhibitio aiheuttaa eksitatorisen ja inhibitorisen neurotransmission epätasapainoa hermosoluverkostoissa, mikä johtaa epileptisiin kohtauksiin.

Neuronien spontaania hermoverkkotason aktiivisuutta voidaan tutkia käyttämällä mikroelektrodi-tekniikkaa (microelectrode arrays, MEAs), jossa kuoppalevyjen kuoppien pohjaan on upotettu mikroelektrodeja. Silti suurin osa elektrofysiologisista tutkimuksista, joita käytetään Dravetin oireyhtymän mallintamiseen hiirimallien avulla, suoritetaan yksisolutasolla. Vaikka tällaiset tutkimukset ovat tärkeitä sairauden synnyn taustalla olevien molekyylitekijöiden määrittämisessä, ne eivät kuvaa miten hermoverkkotason toiminta ilmenee Dravetin oireyhtymässä ja ihmisellä. Siten on olemassa tarve ihmisspesifeille *in vitro*-malleille, jotka hyödyntävät potilasperäisiä ihmisen indusoiduista pluripotenteista kantasoluista (human induced pluripotent stem cell, hiPSC) erilaistettuja neuroneja ja tutkivat näiden neuronien toimintaa MEA-tekniikan avulla.

Tutkimuksessa Dravet-potilasperäinen hiPSC-linja ja kontrolli hiPSC-linja erilaistettiin aivokuoren neuroneiksi ja karakterisoitiin geeni- ja proteiinitasolla käyttämällä kvantitatiivista reaaliaikaista PCR-menetelmää ja immunosytokemiallisia värjäyksiä. Tuotetut neuronit viljeltiin CytoView MEA-kuoppalevyille solujen spontaanin hermoverkkotason aktiivisuuden mittaamiseksi yhteensä 8 viikon ajaksi. Tutkielman tavoitteena oli nähdä ja karakterisoida eroja patologisten ja normaalien terveiden hermosoluverkostojen välillä.

Tutkimuksen tulokset osoittivat, että aivokuoren neuroneiksi erilaistuminen oli tehokasta molemmissa solulinjoissa, luoden soluja, joilla oli kypsän neuronin fenotyyppi ja jotka olivat elektrofysiologisesti aktiivisia MEA-mittauksissa. *SCN1A*-geenin ilmentyminen oli merkittävästi alhaisempi potilassolulinjassa kuin kontrollisolulinjassa. MEA-analyysit paljastivat merkittävän eron hermoverkkoaktiivisuudessa solulinjojen välillä, koska potilaslinjasta peräisin olevat neuronit olivat vähemmän aktiivisia mittausten aikana.

Tästä tutkimuksesta saatua informaatiota voidaan käyttää perustana tulevilla tutkimuksille, jotka suoritetaan Dravet-potilasperäisillä hiPSC-linjoilla MEA-tekniikkaa hyödyntäen. *In vitro*-mallit, joissa käytetään hiPSC-peräisiä neuroneja hermosoluverkoston toiminnan tutkimiseen MEA-tekniikan avulla, ovat lupaava tutkimusalusta epilepsioille, mukaan lukien Dravetin oireyhtymä. Nämä ihmisspesifiset tautimallit voivat edelleen vähentää eläinmallien tarvetta ja käyttöä.

Avainsanat: aivokuoren neuroni, Dravetin oireyhtymä, ihmisen indusoidut pluripotentit kantasolut, mikroelektrodi-tekniikka, natriumkanava, *SCN1A*

PREFACE

This thesis is a part of my Bachelor of Science studies at the Faculty of Medicine and Health Technology (MET) at Tampere University.

I would like to express my gratitude to Adj. Prof. Susanna Narkilahti for giving me the opportunity to work in this project and carry out my Bachelor's thesis in Neuro Group. Special thanks to my supervisor PhD student Ropafadzo Mzezewa, for a great guidance and support during the research work and writing process. I also want to thank all the people in the Neuro Group whom I have worked with during this project. Last, I want to thank my family and friends for their support during this whole process.

Tampere, 26.04.2022

Emma Pesu

ABBREVIATIONS

AEDs	antiepileptic drugs
βIII-tub	βIII-tubulin
DS	Dravet Syndrome
DIV	days in vitro
hPSC	human pluripotent stem cell
hiPSC	human induced pluripotent stem cell
LN521	recombinant human laminin-521
MEA	microelectrode array
MFR	mean firing rate
mwMEA	multi-well microelectrode array
NPC	neural progenitor cell
PEI	poly-ethylene-imide
PLO	poly-L-ornithine
swMEA	single-well microelectrode array

CONTENTS

1. INTRODUCTION

1.1 Epilepsy

Epilepsy is the fourth most common neurological disease estimated to affect around 65 million people worldwide (https://www.epilepsy.com/learn/about-epilepsy-basics/what-epilepsy, viewed 26. January 2022). Characteristic of this brain disorder is predisposition to recurrent epileptic seizures that come together with "neurobiological, cognitive, psychological, and social consequences" (Fisher et al. 2014). At least two unprovoked epileptic seizures have to occur under 24 hours apart according to the definition of epilepsy (Fisher et al. 2014). Abnormal brain function can arise due to either genetic influence or because of varying metabolic and structural brain disorders. Genetic determinants of epilepsy consist of 25% of genes that encode different voltage- and ligand-activated ion channels. Therefore, one of the mechanisms of modern antiepileptic drugs (AEDs) is modulation of the voltage-dependent ion channels. (Kwan et al. 2001; Oyrer et al. 2018) Despite these working AEDs, about one third of patients still have continuous epileptic seizures with poor management due to drug resistance or severe side effects from these drugs (Oyrer et al. 2018; Morrisroe 2019).

Epileptic seizures can manifest in multiple different ways which include motor abnormalities such as involuntary movements or the inability to move, loss of consciousness, and cognitive impairments. Abnormal excessive or synchronous neuronal functionality of the brain is generally the cause of these seizures. (Fisher et al. 2014; Morrisroe 2019) The seizures' extent can vary between focal brain regions and the whole brain level. To discover more about abnormal neurophysiology, approaches using human pluripotent stem cell (hPSC)-derived neurons have shown to be a promising way to model different types of epileptic seizures in vitro. However, animal models have been traditionally the one to which the neurobiological research has relied on so which approach is more valid is a topical question in the field. (Pelkonen et al. 2020; Mzezewa et al. 2022)

Current animal models, for example rodent brain tissue slices, are often considered as "gold standards" for research in drug development and neurotoxicology. Animal-based models have made it possible to discover the essential neurobiological mechanisms in seizures and epilepsy. (Grainger et al. 2018) Therefore, it has been possible to create standards and guidelines to which the future neurobiological research can relate its findings. Although these rodent models have many benefits, for example responding to diverse pharmacological agents and prediction of seizure outcome,

there is debate about the relevance and cost. The lack of human receptors in rodent-utilizing platforms, can produce misleading data because of species-specific differences. (Grainger et al. 2018; Hyvärinen et al. 2019) A promising resolution to these limitations of animal models is hPSC-derived neurons that mimic human cell-specific properties (Pelkonen et al. 2020; Mzezewa et al. 2022). Thus, hPSC-derived neurons provide a human-specific model for in vitro research in neurotoxicity testing, drug screening and disease modeling of epilepsy. In future, they can be as competent model as in vivo animal models and reduce the need and use of animal studies. (Hyvärinen et al. 2019; Mzezewa et al. 2022)

1.1.1 Dravet syndrome

Dravet Syndrome (DS) is a neurodevelopmental disorder associated with a severe form of an early onset epilepsy that begins in childhood within the first year of life. Characteristic of this syndrome are spontaneous convulsive episodes often triggered by fever that continue into adulthood. (Morrisroe 2019) The type and frequency of these seizures can change with aging, being more frequent and severe for the first six years of age and then becoming less frequent and less severe in adolescence (Catterall et al. 2018). Seizures have varying co-morbidities ranging from cognitive and behavioral impairments to motor abnormalities. Mortality rate is high in all age in DS patients. (Genton et al. 2011) Up to 15% of children with DS die prematurely despite of modern diagnosis and treatment options (Catterall et al. 2018). The significant mortality is associated with seizures often being refractory and resistant to the traditional standard AEDs (Catterall et al. 2018).

The fundamental cause of DS is a loss of function of sodium channels and therefore dysregulated action potential firing in cortical GABAergic inhibitory interneurons, the main cell type affected by this syndrome (Yu et al. 2006; Bender et al. 2012). The role of these interneurons is to regulate the excitatory synaptic inputs and outputs of excitatory pyramidal cells via GABA-mediated inhibition. When cortical inhibition is decreased, it causes imbalance of excitatory to inhibitory neurotransmission in neuronal networks that results in epileptic seizure activity. (Ogiwara et al. 2007; Bender et al. 2012) The biological and molecular factors that determine how severe the epileptic seizures can develop into, are not yet fully understood. However, it is known that genetic factors have a great influence in the onset of DS. (Catterall et al. 2018) Approximately 80% of DS patients have mutations in the *SCN1A* gene that is the most common epilepsy gene known so far (Bender et al. 2012; Morrisroe 2019). *SCN1A* gene encodes for the α-subunit of a type I voltage gated sodium channel (Nav1.1) which is responsible of excitability of neurons and thus information transmission throughout the brain (Catterall et al. 2018).

1.2 Sodium channels

Sodium channels are an essential part of properly functioning neuronal networks as they regulate the initiation and propagation of action potentials and information processing in neurons. Each sodium channel has a general structure of one pore-forming α- subunit associated with couple of non-pores forming β-subunits (Ogiwara et al. 2007). The α- subunit of voltage gated sodium channel allows Na^+ ions to cross the cell membrane when a proper change in the cell membrane potential is present. This sodium current depolarizes the cell and affects the burst of an action potential. If the function of this channel is reduced or even lost due to epilepsy-causing mutations, it results in the decrease of sodium currents, disturbances of action potential firing and consequentially spontaneous seizures. (Yu et al. 2006; Morrisroe 2019)

The two main types of SCN1A mutations associated with epilepsy are truncation and missense mutations. Truncation mutation causes a total loss of function and expression of the SCN1A protein and is more represented in patients with DS (Cetica et al. 2017). Missense mutations on the other hand, can change the structure of the protein but often do not affect the most critical part of the protein which is the pore forming region (Cetica et al. 2017). The function and mutations of this neuronal sodium channel have become one of the most important targets for AED action (Kwan et al. 2001). AEDs can function as sodium channel blockers but they aren't always sufficient enough to prevent the epileptic seizures and the disease progression (Catterall et al. 2018). Beside the possible inefficiency of AEDs, one additional problem is the seizures' drug-resistance that one third of the patients suffer. Drug resistance is difficult because it is completely individual which AED can work and if it does not, have previously tried drugs contributed to the alteration of neuronal network behavior which again makes it harder to find a suitable AED combination. (Morrisroe 2019) Early recognition by combination of genetic factors and age together with earlier and more efficient treatment options can in the future limit the progression of DS towards the severe form of it (Cetica et al. 2017).

1.3 Microelectrode arrays

Microelectrode arrays (MEAs) are small chips with embedded microelectrodes in the bottom of the chip. By the help of MEAs, neurons can be cultured on the surface of the electrodes which detect spontaneous or induced neuronal activity by measuring the voltage change of the extracellular culture environment (Morrisroe 2019). There are different kinds of chips with variable spatial resolution able to detect activity from neuronal network level to a single neuron cell. Multi-well MEA (mwMEA) plates resemble traditional cell culture plates with electrodes placed in the bottom of each well whereas single-well MEA (swMEA) plate is based on one well. Both of those formats have varying number of embedded electrodes. mwMEAs are more efficient than single-well MEAs

because with mwMEAs multiple cell cultures can be recorded simultaneously thus reducing the time needed for these experiments. (Cotterill et al. 2016; Morrisroe 2019)

Simultaneously performed recordings with mwMEAs allow a high-throughput approaches in studies of pharmacology and toxicology, and screenings chemicals or disease states for effects on functionality of neurons. Recordings from MEA can be used to describe and characterize the network level functionality of disease-state with patient-derived iPSCs. (Cotterill et al. 2016) Features to be characterized in the neuronal network can be extracellular field potentials described as spikes or bursts when groups of neurons are active (Buzsáki et al. 2012; Pelkonen et al. 2021). Network bursts are the ones that can be detected only from mature neuronal network as network bursts require generation of action potentials in synchrony (Morrisroe 2019). Thus, MEAs are highly effective high-throughput method for enhancing the understanding of communication of neurons as well as a platform for modelling neurological diseases (Hyvärinen et al. 2019; Pelkonen et al. 2020).

Most electrophysiological studies used to model DS in vitro are performed at the single-neuron level but not much is performed at the neuronal network level. There is also variation in whether mouse models or hiPSC are used in these studies. (Higurashi et al. 2013; Favero et al. 2018; Morrisroe 2019) The mouse models using cortical neurons or acute brain slices prepared from mice with Nav1.1 haploinsufficiency have been the most commonly utilized to model DS either on MEAs or using current-clamp electrophysiological recordings (Favero et al. 2018; Morrisroe 2019). The current-clamp is a method used to measure the membrane potential when a simulated current is injected into a cell and it is an ideal technique to evaluate important cellular events, for example action potentials (https://www.moleculardevices.com/applications/patch-clamp-electrophysiology, viewed 29. March 2022). Higurashi et al. conducted current-clamp experiments using DS patient-derived hiPSCs and were the first that successfully generated a human-based in vitro DS model where the electrophysiological behavior of control and patient-derived neurons was examined to a better understanding of DS epileptogenesis (Higurashi et al. 2013). While giving insight into disease pathogenesis, the single-cell level electrophysiological studies, such as the current-clamp, do not describe how neuronal network function is affected in DS. Thus, MEA technology with hPSC-derived neurons from DS patients is needed to study the effects of these neurons on developing and mature neuronal networks. (Cotterill et al. 2016; Favero et al. 2018; Morrisroe 2019)

1.4 Aims of the study

In this thesis Dravet patient derived hiPSC line and control hiPSC line are differentiated into cortical neurons to characterize the differences between “disease-state neurons” and normal healthy neurons by different approaches. Examination of the successfulness of cortical neuron differentiation and the characterization of the cells was conducted at the gene and protein level, after which the functionality was measured with MEAs. The information from this thesis will be used for further studies conducted with Dravet patient derived hiPSC lines.

2. MATERIALS AND METHODS

2.1 Cells

The hPSC lines used in this study consist of the in-house derived hiPSC line 04511.wts and Dravet patient derived hiPSC line DD1C which was received from collaborators Prof. Nicklas Dahl and Jens Schuster from Uppsala University, Sweden (Ojala et al. 2016; Schuster et al. 2019). DD1C line carried distinct *SCN1A* gene mutations (Schuster et al. 2019). Before neural differentiation, hPSCs were transferred and expanded in feeder-free culture on recombinant human laminin-521 (LN521, Biolamina) and E8 medium (Thermo Fisher Scientific) (Hyvärinen et al. 2019). The hPSCs used in this study were acquired from voluntary subjects who had given written and informed consent. The project has supportive statement from Pirkanmaa Hospital District to use the named hPSC lines in neuronal research (R20159). All cultures maintained normal karyotypes and were mycoplasma free.

2.2 Cortical neuron differentiation protocol

The cortical neuronal differentiation protocol was conducted according to a previously published method (Hyvärinen et al. 2019). hPSCs were detached using TrypLE Select (Thermo Fisher Scientific) and plated on poly-L-ornithine (PLO, Sigma) and recombinant human laminin-521-coated well plates in E8 medium containing ROCK inhibitor (Y-27632, Sigma). Neural maintenance medium was used as a basal medium in every stage. During the neural induction stage (days 1-12), the neural maintenance medium was supplemented with LDN193189 (Stemcell Technologies) and SB431542 (Sigma), and the medium was changed daily. At day 12, the cells were detached with StemPro Accutase (Thermo Fisher Scientific) and plated on PLO and LN521-coated well plates in neural induction medium containing ROCK inhibitor. For neural proliferation (days 13-25), the neural maintenance medium was supplemented with fibroblast growth factor-2 (FGF2, R&D Systems),

and the medium was changed every two days. At days 17, 21 and 25, the neural progenitor cells were passaged with StemPro Accutase and replated in neural proliferation medium containing ROCK inhibitor. For final maturation (days 26-67), the medium was changed to neural maintenance medium supplemented with brain-derived neurotrophic factor (BDNF, R&D Systems), glial-derived neurotrophic factor (GDNF, R&D Systems), dibutyryl-cyclic AMP (db-cAMP, Sigma) and ascorbic acid (AA, Sigma). At day 32, the cells were plated for experiments at a density of 50 000 cells/cm^2 on plastic well plates and 635 000 cells/cm^2 on the MEA well plates. Each of MEA plates contained 48 well chambers with 16 electrodes per well. Plastic well plates were coated with PLO and LN521 as before and MEA well plates with poly-ethylene-imide (PEI, Sigma) and LN521. Medium changes were performed every other day.

2.3 RNA isolation and quantitative real-time PCR

RNA was collected from well plates at timepoints 12, 17, 21, 25, 32, 46 and 67 days in vitro (DIV). RNA was isolated and purified using NucleoSpin RNA kit (Macherey-Nagel, cat no: 2101/001). The concentration and purity of RNA samples were quantified with a NanoDrop 1000 (Thermo Fisher Scientific). After RNA isolation, cDNA was synthesized using High Capacity cDNA Reverse Transcription Kit (Applied Biosystems cat no: 4368814) from 200 ng of total RNA. Quantitative real-time PCR was performed by QuantStudio 12K Flex Real-Time PCR System with 5 ng of the cDNA with primers βIII-tub (Hs00801390_s1), SCN1A (Hs00374696_m1) and GAPDH (Hs99999905_m1). βIII-tubulin (βIII-tub) is a neuronal specific gene, SCN1A is a gene that encodes the type 1 neuronal voltage-gated sodium channel and GAPDH is a housekeeping gene. The data is presented with relative quantification (RQ) values by GraphPad Prism software from three samples (n= 3) per group. A Mann-Whitney U-test was used to determine statistical significance of the βIII-tubulin and SCN1A expression between the two cell lines at different timepoints.

2.4 Immunocytochemical stainings

Immunocytochemistry was performed according to Lappalainen et al., 2010, at timepoints 12, 21, 32, 46 and 67 DIV (Lappalainen et al. 2010). Briefly, the cell samples were blocked with 10% normal donkey serum, 0.1% TritonX-100 and 1% bovine serum albumin in PBS, at room temperature for 45 min. The samples were then incubated with mixture of primary antibodies overnight at +4°C. Primary antibodies consisted of βIII-tubulin (βIII-tub) (mouse, 1:1000), FOXG1 (rabbit, 1:500), GFAP (chicken, 1:4000), MAP2 (chicken, 1:4000), MAP2 (rabbit, 1:400), Pax6 (rabbit, 1:1000), Sox2 (mouse, 1:200) and Vimentin (mouse, 1:500). FOXG1, Pax6 and Sox2 antibodies were used to detect early neuroectodermal proteins. βIII-tubulin and MAP2 were used as neuronal specific antibodies, βIII-tubulin was for detecting neuronal axon protein and MAP2 for detecting neuronal dendrite protein. GFAP was used to detect astrocytes and Vimentin to detect neural stem and

progenitor cells. After overnight primary antibody incubation, the samples were incubated at room temperature for an hour with fluorescent labeled secondary antibodies: Alexa Fluor 488 (1:400), Alexa Fluor 568 (1:400) or Alexa Fluor 647 (1:200) dyes (all from Thermo Fisher Scientific). The cells were imaged using an Olympus IX51 fluorescence microscope (Olympus Corporation, Hamburg, Germany).

2.5 Microelectrode array measurements

Neuronal network activity was recorded with an Axion Maestro system controlled by AxIS software (Axion Biosystems). The start of MEA experiments was DIV 32 when cells were plated for culturing and MEA plates as described above. Thereafter, cultures were kept in neural maturation medium and cultured at + 37 °C in a 5% CO_2 humidified incubator. Medium changes were performed four times a week. For recording spontaneous activity development, CytoView MEA 48 well plates were used (Axion Biosystems). CytoView MEA 48 well plate contained 14 wells for DD1C and 10 wells for control line 04511.wts derived neurons**.** Recordings were performed under 37°C temperature control and a time period of 10 min. MEA plates were allowed to equilibrate for 5 min prior to any recordings. Spontaneous activity of the neurons was measured twice a week for 10 min for a total of 8 weeks. The data was analyzed by an in-house-made script described in Hyvärinen et al. 2019. A Mann-Whitney U-test was used to compare differences between the 04511.wts (n= 10) and DD1C (n= 14) lines at different timepoints.

3. RESULTS

3.1 Characterization of cells

3.1.1 Gene level characterization

To quantify the relative amount of target nucleic acid and to compare the expression of target genes between hiPSC lines 04511.wts and DD1C derived neurons, quantitative real-time PCR was conducted. The DD1C hiPSC line derived neurons are here on defined as DD1C group, and the control hiPSC line 04511.wts derived neurons as control group. The quantification data is based on relative quantification (RQ) values. The RQ value is defined as fold change compared to the calibrator which is the sample that all others are compared to. (https://genomique.iric.ca/resources/files/How_to_deal_with_qPCR_results.pdf, viewed 2. April 2022) In Figure 1, the calibrator was βIII-tubulin at DIV 12 for each group separately and in Figure 2 it was SCN1A at DIV 12 of the control group for both groups.

The RQ values of βIII-tubulin between the control and DD1C groups at different timepoints can be seen in Figure 1. On DIV 12, which was the calibrator sample, the RQ value was 1 for both groups. After that timepoint, a lot of variation appeared in the relative amount of βIII-tubulin depending on the group and timepoint. On DIV 46, the RQ value of the control group was approximately 9, meaning that βIII-tubulin was 9 times more expressed in the samples than in the calibrator sample on DIV 12. Instead with the DD1C group, the highest expression of βIII-tubulin was detected on DIV 67 as the RQ value was approximately 6. Thus, in the control group βIII-tubulin was expressed earlier than in the DD1C group and with greater amounts of the gene. Statistically significant ($p < 0.05$) difference in the expression of βIII-tubulin between the groups was found on DIV 32, 46 and 67. Interestingly, the expression level of βIII-tubulin gene in the control group decreased during DIV 46 and 67 whereas in the DD1C group the increase of βIII-tubulin expression levels was consistent during the same time period.

In Figure 2, the RQ values of SCN1A are presented between the control and DD1C groups at the same timepoints as in Figure 1. The calibrator sample was control group on DIV 12, so the RQ value of the control group on DIV 12 was 1 and the RQ value of DD1C group was approximately 3. On DIV 21, the RQ values of both groups were around value 0.5, meaning that the SCN1A gene was 5 times less expressed than in the calibrator sample on DIV 12. At all other timepoints, the expression of SCN1A was yet increased in both groups. On DIV 46, the RQ value of the control group was approximately 70, meaning that the SCN1A was 70 times more expressed on DIV 46 than on DIV 12. The SCN1A expression of DD1C group didn’t reach as high levels as in control group. In DD1C group, the SCN1A expression was as its highest on DIV 67 as the RQ value was approximately 20. Statistically significant ($p < 0.05$) difference in the expression of SCN1A between the groups was found on DIV 32, 46 and 67 showing that the control group was expressing more the SCN1A gene than the DD1C group during the neuronal maturation.

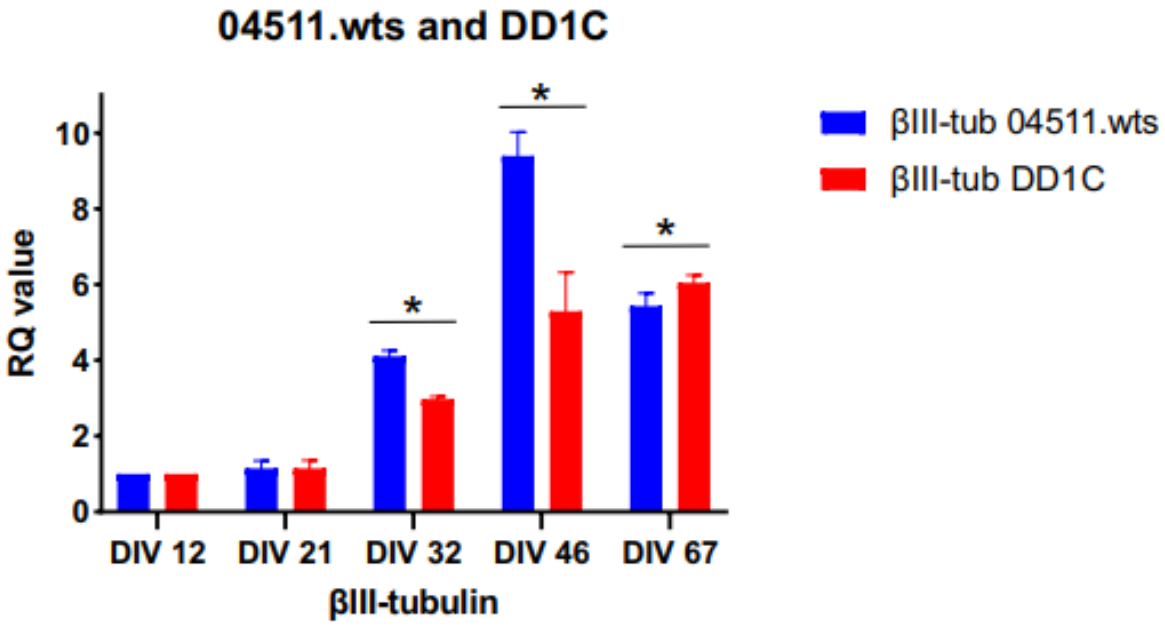

Figure 1. Graph is presenting means of the RQ values from three samples per group with error whiskers presenting standard deviation (SD). The RQ value is indicating the relative quantification of βIII-tubulin and it is presented between the control and DD1C groups from DIV 12 to 67. Mann-Whitney U test was performed to compare differences between the groups at each time point, and significance is marked as *p<0.05.

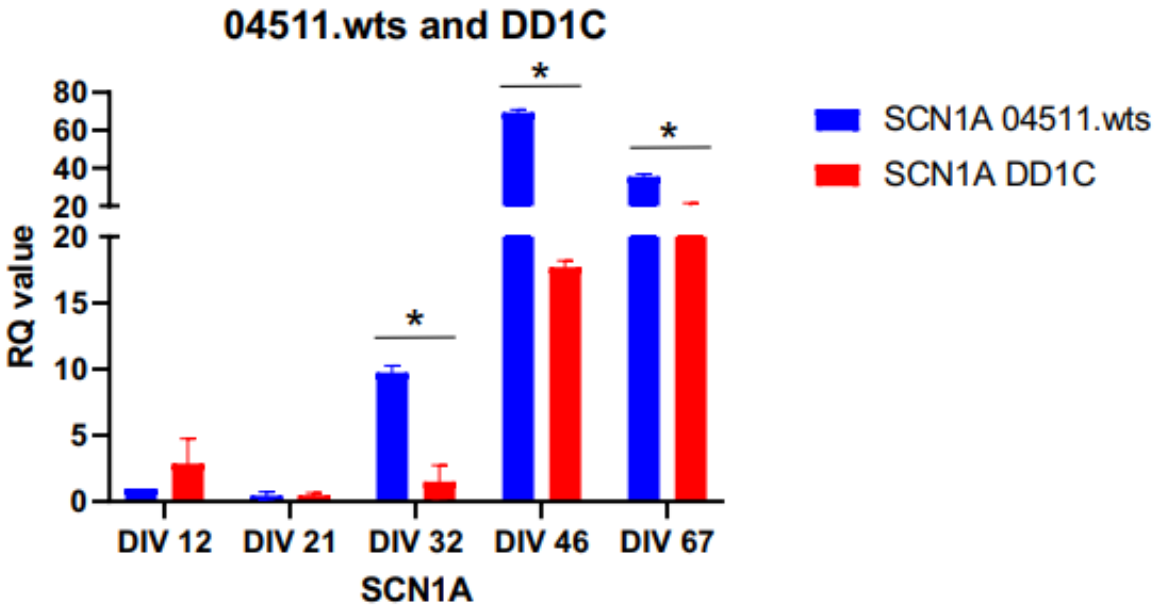

Figure 2. Graph is presenting means of the RQ values from three samples per group with error whiskers presenting standard deviation (SD). The RQ value is indicating the relative quantification of SCN1A and it is presented between the control and DD1C groups from DIV 12 to 67. Mann-Whitney U test was performed to compare differences between the groups at each time point, and significance is marked as *p<0.05.

3.1.2 Protein level characterization

The successfulness of the cortical neuron differentiation at different stages was assessed by immunocytochemical stainings on DIV 12, 21, 32, 46 and 67 in the control and DD1C groups. On DIV 12, after the neural induction by dual SMAD inhibition, the cells were characterized with early neuroectodermal markers Sox2 and Pax6 for their efficiency to becoming neuroectodermal cells. Both groups showed expression of Sox2 and Pax6, indicating efficient neural conversion (Figure 3). After the neural induction stage on DIV 21, the cells expressed neuroectodermal markers FoxG1 and Pax6 but the expression of dendrite marker MAP2 wasn't so high which indicated the presence of cells that had anterior cortical fate but yet no growing neurites (Figure 4). In addition, Vimentin-positive neural progenitor cells (NPCs) emerged at this timepoint of differentiation. Stainings showing Pax6 and Vimentin expressing neural stem and progenitor cells were a promising result that the neuronal differentiation was proceeding as NPCs can differentiate into mature neural cell types which are neurons and astrocytes (Figure 4).

MAP2, βIII-tub and GFAP stainings were performed during neuronal maturation from DIV 32 to 67. MAP2 and βIII-tub markers were used to evaluate the emergence of neurons and GFAP to evaluate the emergence of astrocytes. The presence of MAP2 and βIII-tub positive neurons and GFAP positive astrocytes increased with time in the control and DD1C groups (Figure 5, 6). Particularly noticeable difference in the expression happened with neurons expressing βIII-tub and astrocytes expressing GFAP. In Figure 5 on DIV 32, neurons with axonal projections were already noticeable in both groups indicating the start of neuronal network formation. On DIV 46 and 67, the complex neuronal networks with paths and connections between the neurons were identified by MAP2 and βIII-tub stainings (Figure 6). On DIV 32, the expression of GFAP looked more like a background from the stainings and individual cells expressing astrocytic markers were almost impossible to detect (Figure 5). Thus, the development of astrocytes was as its highest from DIV 46 to 67 as can be seen in Figure 6. The highest expression of GFAP was detected on DIV 67 as the emergence of individual astrocytes expressing GFAP were possible to be observed (Figure 6). These results showed that the neuronal differentiation was successful in the control group and DD1C group.

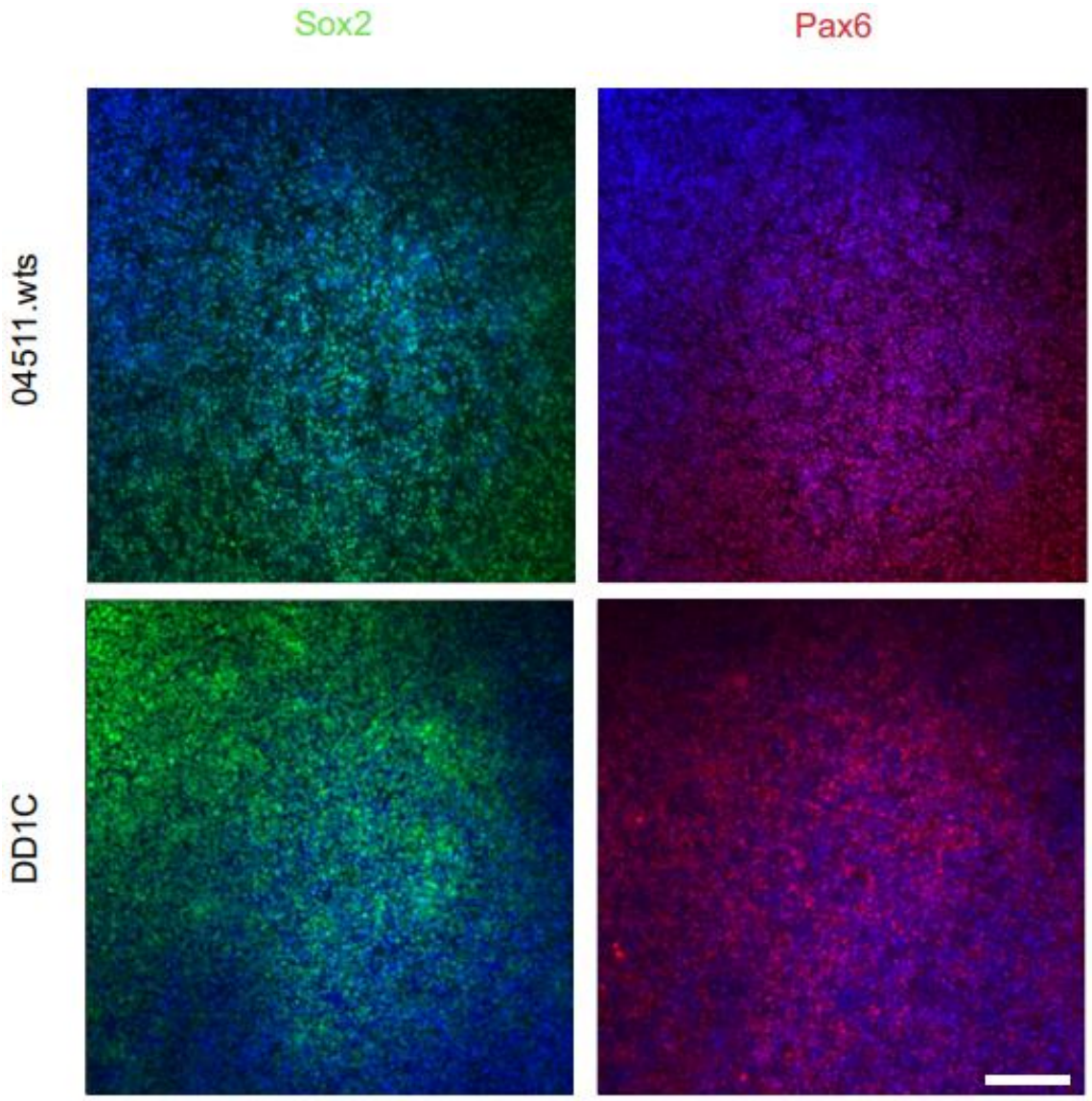

Figure 3. The control group and DD1C group were characterized for their efficiency to becoming neuroectodermal cells after 12-day neural induction by dual SMAD inhibition. Early neuroectodermal markers Sox2 and Pax6 were used to evaluate the presence of neuroectodermal cells. Dapi nuclear staining is shown in blue, and the scale bar is 100 μm.

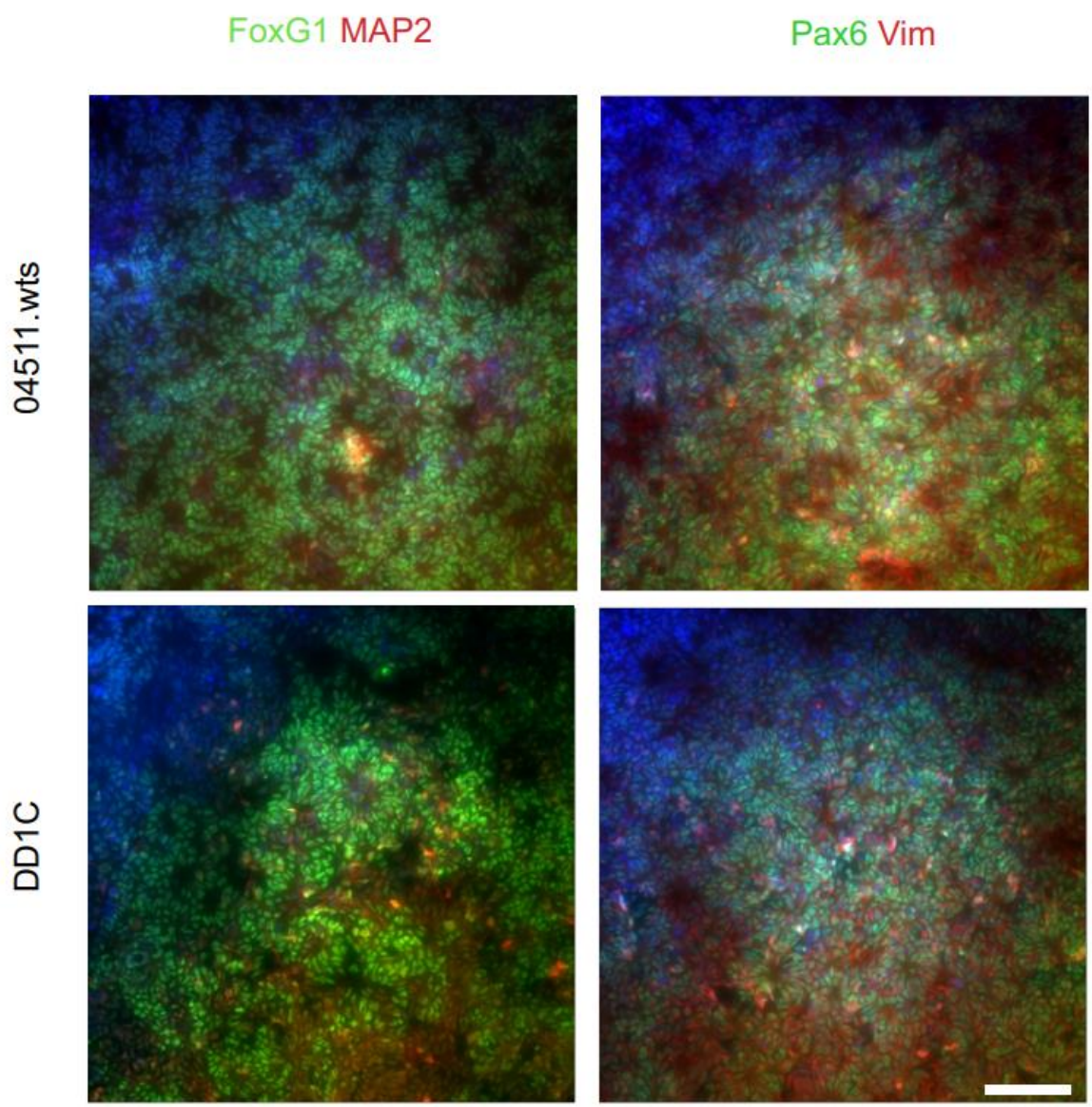

Figure 4. Fluorescence images of the control group and DD1C group after 21 days of differentiation. The cells were characterized with dendrite marker MAP2, neural stem cell marker Vimentin (Vim) and with neuroectodermal markers FOXG1 and Pax6, to assess the presence of neural progenitor and neural stem cells. Dapi nuclear staining is shown in blue and, the scale bar is 100 μm.

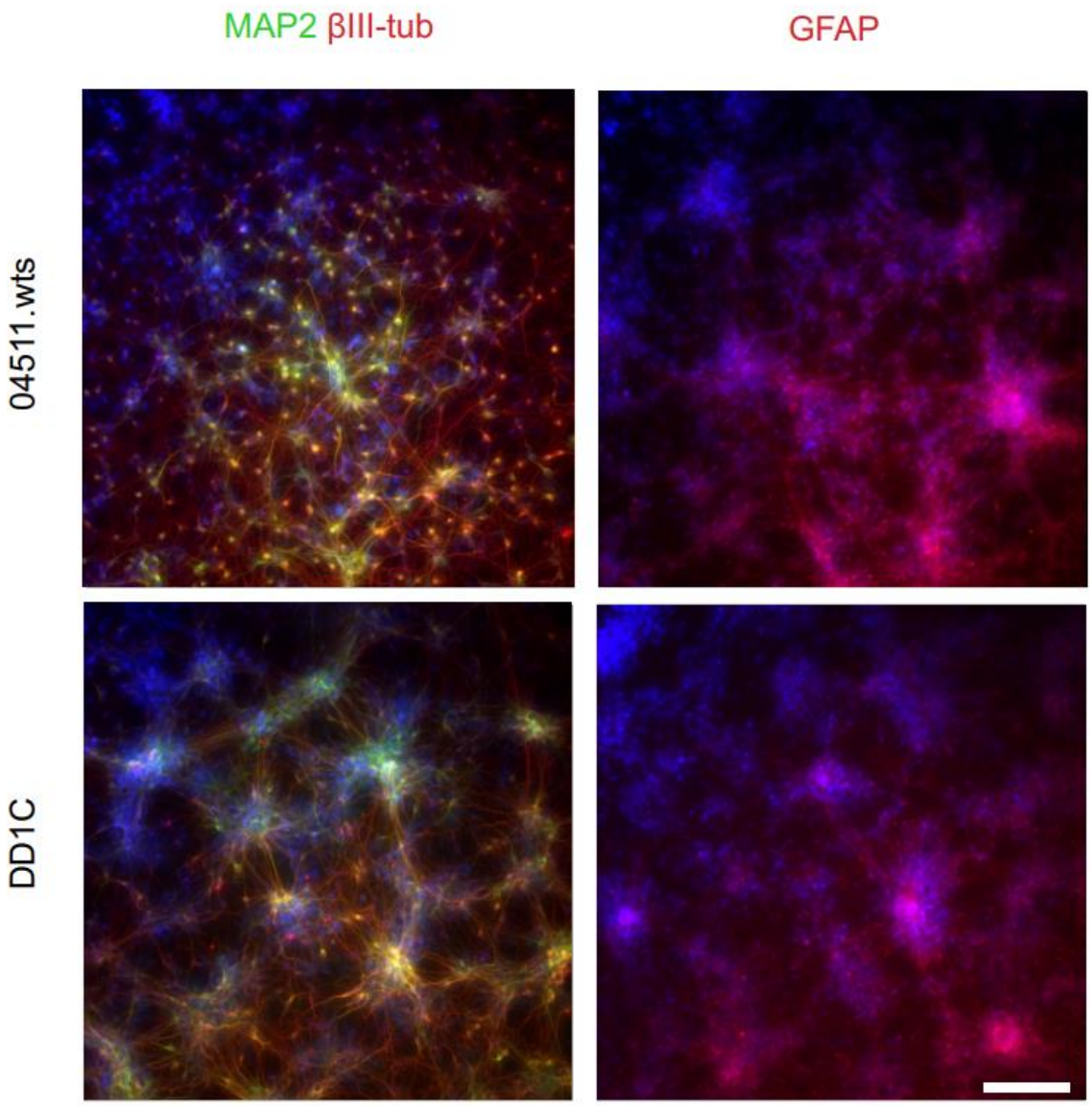

Figure 5. Fluorescence images of maturing neurons (MAP2 and βIII-tubulin) and astrocytes (GFAP) on day 32 of differentiation in the control group and DD1C group. Dapi nuclear staining is shown in blue and, the scale bar is 100 μm.

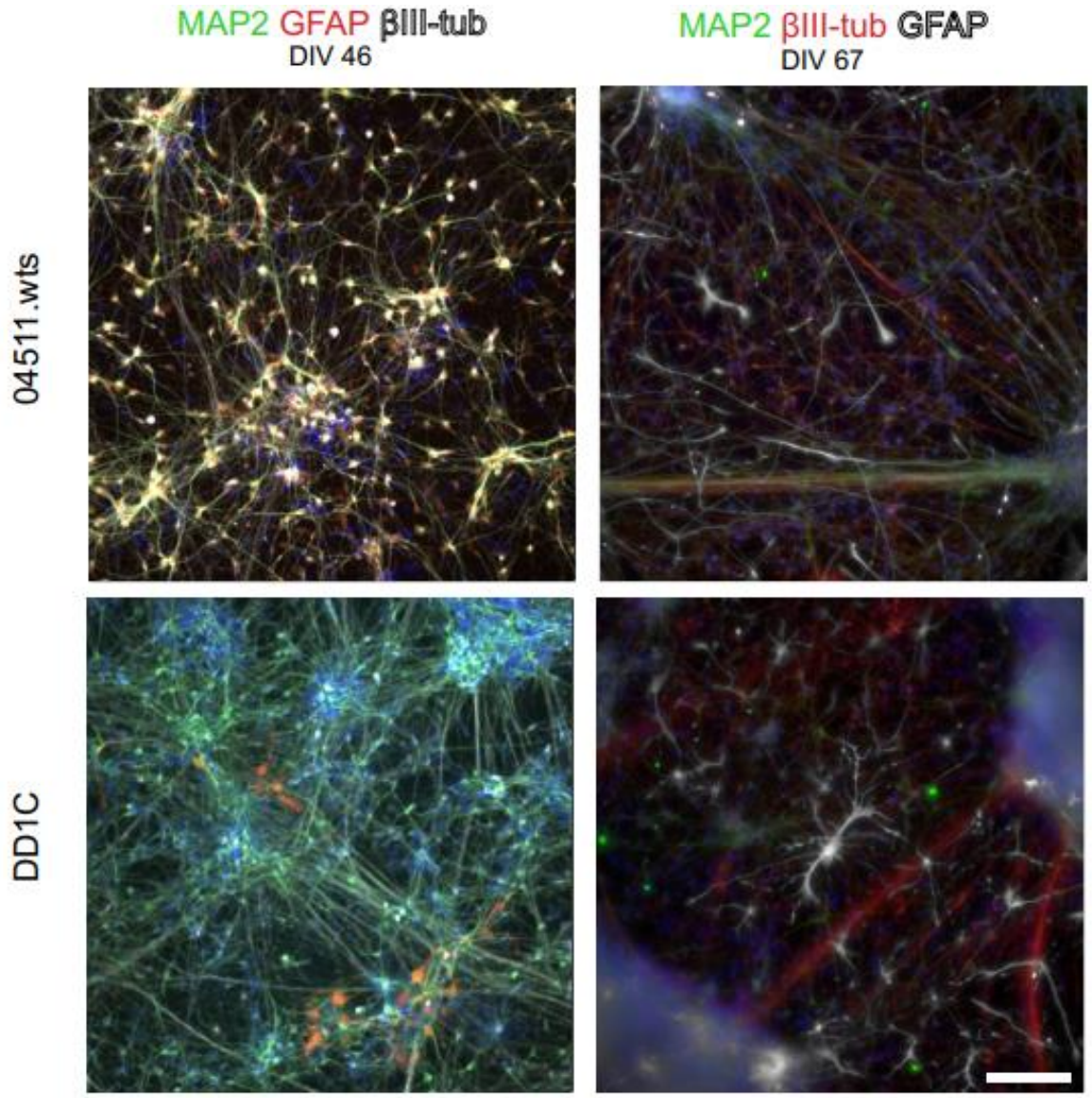

Figure 6. Fluorescence images of neurons (MAP2 and βIII-tub) and astrocytes (GFAP) on DIV 46 and 67 in the control group and DD1C group. Dapi nuclear staining is shown in blue and, the scale bar is 100 ųm.

3.2 Electrophysiological functionality of cells

To assess the electrophysiological functionality and to compare the possible differences of that between the control group and DD1C group, MEA recordings were performed twice a week from DIV 35 until DIV 90, using the recording protocols and the analysis tools described earlier. MEA data can be examined using different parameters that represent either spike activity, bursting activity or network connectivity in the neuronal cultures (Morrisroe 2019). In this study, burst rate that represents the number of bursts per minute and the mean firing rate (MFR) that represents spiking activity of the active electrodes, were chosen to assess the total network activity. In Figure 7, the burst rate increased considerably over time in the control group but in DD1C group, the increase

of burst rate wasn't as high and remained relatively constant during the same time. Beside different levels of burst rate, also the peaks of bursts varied a lot between the groups. In the control group, peaking was detected at DIV 60 with a rate of 13 Hz and in DD1C at DIV 41 with a rate of 5 Hz (Figure 7). Statistically significant difference ($p < 0.001$) in the burst rate between the control and DD1C neuronal networks was found on DIV 60, 62 and 74.

Similarly the mean firing rate of active electrodes increased more in the control group and reached a peak rate of 4 Hz at DIV 60 whereas the mean firing rate of the DD1C group didn't reach as distinct peak rate at any timepoint (Figure 8). In addition, in DD1C group the mean firing rate levels of active electrodes were less than a 2 Hz during all the recording timepoints (Figure 8). Statistically significant difference ($p < 0.001$) in the mean firing rate between the groups was found similarly on DIV 60, 62 and 74 as in the burst rate. Thus, the network activity development of the control group was greater than in DD1C group after almost 4 weeks on MEA. In the control group, **t**he neurons were more electrophysiologically active creating synchronous bursts more often.

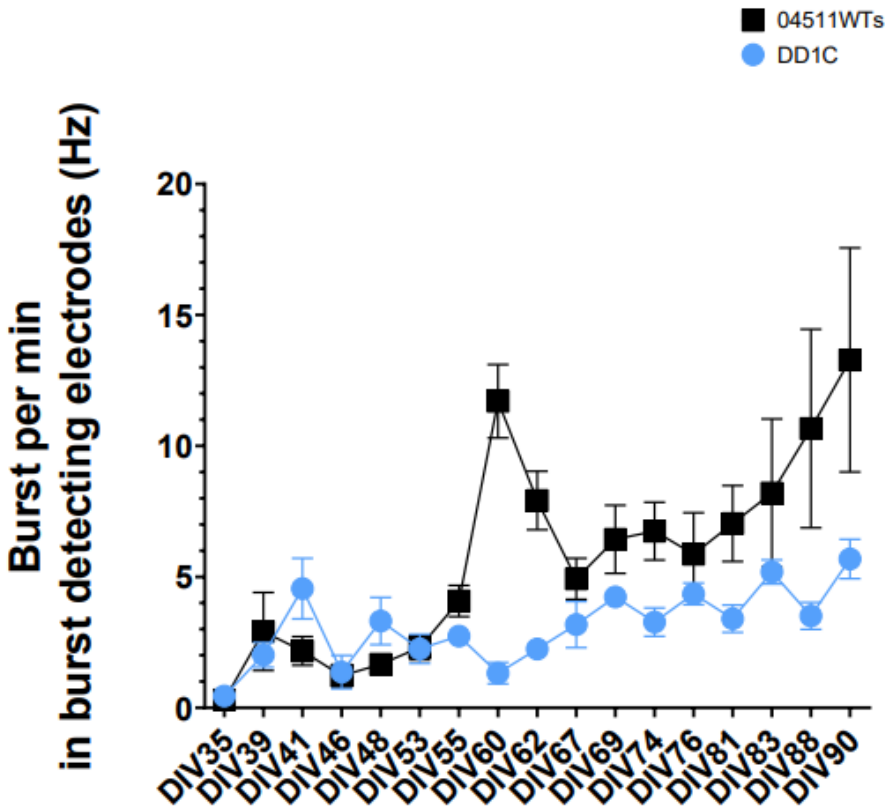

Figure 7. Graph is presenting means of the number of bursts per minute in burst detecting electrodes (Hz) with error whiskers presenting standard deviation (SD). Changes in burst rate show the electrophysiological activity development of the control group and DD1C group over time.

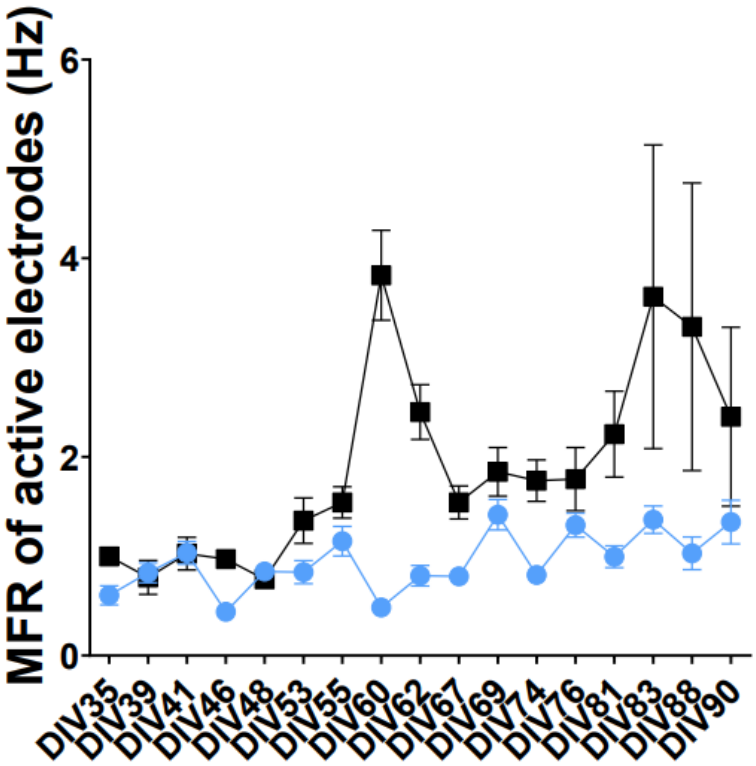

Figure 8. Graph is presenting means of the mean firing rate (MFR) of active electrodes (Hz) with error whiskers presenting standard deviation (SD). Changes in mean firing rate show the electrophysiological activity development of the control group and DD1C group over time.

4. DISCUSSION

In the study, differentiation of the DS patient derived hiPSC line and control hiPSC line into cortical neurons was conducted according to Hyvärinen et al. 2019. The generated neurons were characterized at the gene and protein level and plated on CytoView MEA 48 well plates to record the neuronal network activity for a total of 8 weeks. Spontaneous electrophysiological activity of the neurons was analyzed by parameters that represent spike and bursting activity in the neuronal cultures.

Immunocytochemical analysis demonstrated that the control 04511.wts and the patient DD1C cell lines successfully differentiated into cortical neurons of typical character. After 12-day neural induction by dual SMAD inhibition, both of the studied groups expressed early neuroectodermal markers Sox2 and Pax6 showing efficient neural conversion. After the neural induction stage on

DIV 21, the cells expressed FoxG1 which indicated the anterior cortical fate of the cells but the expression of dendrite marker MAP2 wasn't so high as previously reported in this stage of differentiation (Hyvärinen et al. 2019). The lower expression of MAP2 can be due to slower neuronal maturation rate of the used hiPSC lines in this study. In addition, the expression of Vimentin and Pax6 was apparent indicating the presence of neural stem and progenitor cells as reported earlier in Hyvärinen et al. The emergence of neuroprogenitors is also supported by the formation of neural rosettes on DIV 21 as the NPCs within neural rosettes express many of the proteins expressed in neuroepithelial cells and can differentiate into neurons (Wilson and Stice 2006). During time period of DIV 32-67, the increased appearance of neurite markers βIII-tubulin and MAP2 expressing cells suggested efficient neuronal maturation as mature neuronal morphology includes a large and complex cell body and growth of ≥4 neurites (Higurashi et al. 2013). The appearance of GFAP-expressing astrocytes similarly increased during this same time period suggesting subsequent astrogenesis from the NPCs as detected in the study by Hyvärinen et al. The formation of astrocytes showed successful differentiation into mature neural cell types in the control and DD1C groups as astrocytes are important contributing factor of synaptogenesis and functional maturation of neurons (Hyvärinen et al. 2019).

The expression of neuronal βIII-tubulin gene increased consistently during the neuronal differentiation in both studied groups, indicating that the cells were differentiating and maturing into neurons. The highest expression levels of βIII-tubulin gene in the control group and DD1C group were detected between DIV 32 and 67 which was also seen at the protein level in the immunocytochemical staining analysis. Comparison of the βIII-tubulin expression levels between the groups revealed that the βIII-tubulin gene was significantly more expressed in the control group on DIV 32 and 46 than in the DD1C group. Similarly, the expression of SCN1A gene was significantly higher in the control group from DIV 32 to 67, indicating that the DD1C group with a distinct SCN1A gene mutations didn't have a normal SCN1A gene expression.

In the study, electrophysiological comparison between the studied groups showed that overall the spontaneous network level activity of the DD1C group was significantly lower than the activity of control group. Both mean firing rate and burst rate levels were significantly lower in DD1C networks than in 04511.wts networks. In contrast, in the study conducted with DS mouse counterparts by Morrisroe, the typical profile of epileptic neuronal networks in mouse included significantly lower burst rate but significantly higher mean firing rate. These results reflect the inhibited activity of GABAergic interneurons when networks on MEA contain a high amount of these interneurons (Morrisroe 2019). However in this study, the DD1C group had significantly reduced mean firing and bursting rates that is not the profile expected for epileptic networks according to mouse models of DS (Morrisroe 2019). This can be due to a lower amount of inhibitory GABAergic interneurons in

neuron populations as the activity of neuronal cultures is often produced by excitatory glutamatergic neuronal networks (Hyvärinen et al. 2019). Another possible factor explaining the result that DS patient line derived neurons were not as electrophysiologically active on MEAs as the control neurons, is that the DD1C group didn't mature as much. This is supported by the expression levels of the neuronal βIII-tubulin gene which were significantly lower in DD1C group than in the control group during neuronal maturation.

In the study, the activity development of the hiPSC line 04511.wts derived neuronal networks were very similar to the results detected by Hyvärinen et al, in hPSC-derived neuronal networks. The activity peak of 04511.wts networks was reached on DIV 60 with a spike rate of 4 Hz whereas the activity peak of hPSC-derived networks was reached on DIV 56 with a spike rate of 4.4 Hz per well (Hyvärinen et al. 2019). In addition, both hiPSC and hPSC-derived networks showed a progressive increase in the number of bursts (Hyvärinen et al. 2019). Spontaneous bursts are important for the formation of neuronal networks due to which they often emerge during early activity development of the cerebral cortex (Hyvärinen et al. 2019). Thus, the MEA measurements demonstrated that the control line 04511.wts derived neurons matured into electrophysiologically active cortical neurons. The spontaneous activity was detected also from the patient line DD1C derived neurons but more studies need to be performed using DS patient derived iPSCs on MEAs to study the epileptic network level activity.

5. CONCLUSIONS

The differentiation and characterization of DS patient derived hiPSC line and control hiPSC line into cortical neurons was successful. The neural induction of hiPSCs and expansion and maturation of produced cells was efficient as the cells represented a mature neuron phenotype. According to gene expression analysis, the expression on neuronal specific gene βIII-tubulin was increased in both groups during neuronal maturation and the expression levels of SCN1A were significantly higher in the control group than in DD1C group. Electrophysiological functionality significantly differed between the groups as the neuronal networks of the control group were more active than the DD1C networks. The results are beginning of utilization of models that use hiPSC-derived neurons from DS patients on MEAs. These models can be used in human epilepsy research but more studies need to be performed to create standards and guidelines for the repeatability and reliability of these in vitro human-specific models.

REFERENCES

Bender, A. C., Morse, R. P., Scott, R. C., et al. (2012). SCN1A mutations in Dravet syndrome: Impact of interneuron dysfunction on neural networks and cognitive outcome. *Epilepsy & Behavior*, *23*(3), 177–186.

Buzsáki, G., Anastassiou, C. A., & Koch, C. (2012). The origin of extracellular fields and currents—EEG, ECoG, LFP and spikes. *Nature Reviews Neuroscience*, *13*(6), 407–420.

Catterall, W. A. (2018). Dravet syndrome: A sodium channel interneuronopathy. *Current Opinion in Physiology*, *2*, 42–50.

Cetica, V., Chiari, S., Mei, D., et al. (2017). Clinical and genetic factors predicting Dravet syndrome in infants with *SCN1A* mutations. *Neurology*, *88*(11), 1037–1044.

Cotterill, E., Hall, D., Wallace, K., et al. (2016). Characterization of Early Cortical Neural Network Development in Multiwell Microelectrode Array Plates. *Journal of Biomolecular Screening*, *21*(5), 510–519.

Favero, M., Sotuyo, N. P., Lopez, E., et al. (2018). A Transient Developmental Window of Fast-Spiking Interneuron Dysfunction in a Mouse Model of Dravet Syndrome. *The Journal of Neuroscience*, *38*(36), 7912–7927.

Fisher, R. S., Acevedo, C., Arzimanoglou, A., et al. (2014). ILAE Official Report: A practical clinical definition of epilepsy. *Epilepsia*, *55*(4), 475–482.

Genton, P., Velizarova, R., & Dravet, C. (2011). Dravet syndrome: The long-term outcome: Long-Term Outcome. *Epilepsia*, *52*, 44–49.

Grainger, A. I., King, M. C., Nagel, D. A., et al. (2018). In vitro Models for Seizure-Liability Testing Using Induced Pluripotent Stem Cells. *Frontiers in Neuroscience*, *12*, 590.

Higurashi, N., Uchida, T., Lossin, C., et al. (2013). A human Dravet syndrome model from patient induced pluripotent stem cells. *Molecular Brain*, *6*(1), 19.

Hyvärinen, T., Hyysalo, A., Kapucu, F. E., et al. (2019). Functional characterization of human pluripotent stem cell-derived cortical networks differentiated on laminin-521 substrate: Comparison to rat cortical cultures. *Scientific Reports*, *9*(1), 17125.

Kwan, P., Sills, G. J., & Brodie, M. J. (2001). The mechanisms of action of commonly used antiepileptic drugs. *Pharmacology & Therapeutics*, *90*(1), 21–34.

Lappalainen, R. S., Salomäki, M., Ylä-Outinen, L., et al. (2010). Similarly derived and cultured hESC lines show variation in their developmental potential towards neuronal cells in long-term culture. *Regenerative Medicine*, *5*(5), 749–762.

Morrisroe, E. (n.d.). *MULTIELECTRODE ARRAYS: A TOOL FOR MODELLING GENETIC EPILEPSY*. 151.

Mzezewa, R., Lotila, J., Kiiski, H., et al. (2022). A kainic acid-induced seizure model in human pluripotent stem cell-derived cortical neurons for studying the role of IL-6 in the functional activity. *Stem Cell Research*, *60*, 102665.

Ogiwara, I., Miyamoto, H., Morita, N., et al. (2007). Nav1.1 Localizes to Axons of Parvalbumin-Positive Inhibitory Interneurons: A Circuit Basis for Epileptic Seizures in Mice Carrying an Scn1a Gene Mutation. *Journal of Neuroscience*, *27*(22), 5903–5914.

Ojala, M., Prajapati, C., Pölönen, R.-P., et al. (2016). Mutation-Specific Phenotypes in hiPSC-Derived Cardiomyocytes Carrying Either Myosin-Binding Protein C Or *α* -Tropomyosin Mutation for Hypertrophic Cardiomyopathy. *Stem Cells International*, *2016*, 1–16.

Oyrer, J., Maljevic, S., Scheffer, I. E., et al. (2018). Ion Channels in Genetic Epilepsy: From Genes and Mechanisms to Disease-Targeted Therapies. *Pharmacological Reviews*, *70*(1), 142–173.

Pelkonen, A., Mzezewa, R., Sukki, L., et al. (2020). A modular brain-on-a-chip for modelling epileptic seizures with functionally connected human neuronal networks. *Biosensors and Bioelectronics*, *168*, 112553.

Pelkonen, A., Pistono, C., Klecki, P., et al. (2021). Functional Characterization of Human Pluripotent Stem Cell-Derived Models of the Brain with Microelectrode Arrays. *Cells*, *11*(1), 106.

Schuster, J., Fatima, A., Sobol, M., et al. (2019). Generation of three human induced pluripotent stem cell (iPSC) lines from three patients with Dravet syndrome carrying distinct SCN1A gene mutations. *Stem Cell Research*, *39*, 101523.

Wilson, P. G., & Stice, S. S. (2006). Development and differentiation of neural rosettes derived from human embryonic stem cells. *Stem Cell Reviews*, *2*(1), 67–77.

Yu, F. H., Mantegazza, M., Westenbroek, R. E., et al. (2006). Reduced sodium current in GABAergic interneurons in a mouse model of severe myoclonic epilepsy in infancy. *Nature Neuroscience*, *9*(9), 1142–1149.